Stable double-resonance optical spring in laser gravitational-wave detectors

Andrey A. Rakhubovsky,[1] Stefan Hild,[2] and Sergey P. Vyatchanin[1]

[1]*Physics Department, Moscow State University, Moscow 119992 Russia*
[2]*SUPA, School of Physics and Astronomy, University of Glasgow, Glasgow, Q12 8QQ, United Kingdom*

We analyze the optical spring characteristics of a double pumped Fabry-Perot cavity. A double-resonance optical spring occurs when the optical spring frequency and the detuning frequency of the cavity coincide. We formulate a simple criterion for the stability of an optical spring and apply it to the double-resonance regime. Double-resonance configurations are very promising for future gravitational-wave detectors as they allow us to surpass the Standard Quantum Limit. We show that stable double resonance can be demonstrated in middle scale prototype interferometers such as the Glasgow 10 m-Prototype, Gingin High Optical Power Test Facility or the AEI 10 m Prototype Interferometer before being implemented in future gravitational-wave detectors.

I. INTRODUCTION

Currently the search for gravitational radiation from astrophysical sources is conducted with the first-generation Earth-based laser interferometers (LIGO in USA [1–3], VIRGO in Italy [4,5], GEO-600 in Germany [6,7], TAMA-300 in Japan [8,9], and ACIGA in Australia [10,11]). The development of the second-generation gravitational-wave (GW) detectors (Advanced LIGO [12,13], Advanced Virgo [14], GEO-HF [15], and LCGT [16]) is well underway.

The sensitivity of the first-generation detectors is limited by noises sources of various nature: seismic and suspension thermal noise at low frequencies (below ∼50 Hz), thermal noise in suspensions, bulks and coatings of the mirrors (∼ 50–200 Hz), photon shot noise (above ∼200 Hz). It is expected that the sensitivity of the second-generation detectors will be ultimately limited by the noise of quantum nature arising due to Heisenberg's uncertainty principle [17–20] over most of the frequency range of interest. The optimum between measurement noise (photon shot noise) and back-action noise (radiation pressure noise) is called the Standard Quantum Limit (SQL). This level is expected to be reached in the forthcoming second generation of large-scale laser-interferometric gravitational-wave detectors. Third-generation detectors, such as the Einstein Telescope [21] aim to significantly surpass the SQL over a wide frequency range [22].

The most promising methods to overcome the SQL rely on the implementation of optical (ponderomotive) rigidity [20,23–25], which effectively turns the test masses of a gravitational-wave detector into harmonic oscillators producing a gain in sensitivity [26–31]. In order to understand it, note that the formula for the sensitivity $\xi(\Omega)$ of Advanced LIGO interferometer (see Fig. 1) consists of two terms:

$$\xi^2(\Omega) = \frac{S_h(\Omega)}{h_{\mathrm{SQL}}^2(\Omega)}$$
$$= \frac{2}{\hbar m \Omega^2}(S_F(\Omega) + \mu^2|K(\Omega) - \Omega^2|^2 S_x(\Omega)). \quad (1)$$

Here S_h is the total single-sided spectral density of the noise recalculated to the strain density h of the gravitational wave $h_{\mathrm{SQL}}^2 = 2\hbar/\mu L^2 \Omega^2$—the value of S_h corresponds to the SQL sensitivity for the case of free masses, Ω is the observation frequency, L the arm length of the
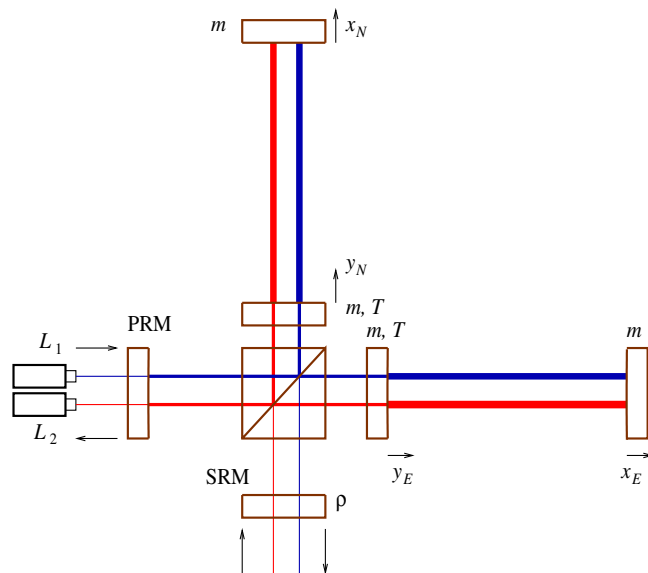

FIG. 1 (color online). Scheme of an Advanced LIGO interferometer pumped by two lasers. The main laser is detuned to give a positive optical rigidity and negative damping (it is tuned on the right slope of resonance curve), while the auxiliary laser is detuned to give negative optical rigidity and positive damping.

interferometer, $\mu = m/4$ is the reduced mass, m is the mass of each mirror of the arm cavities, S_x and S_F are the single-sided spectral densities of the measurement noise and the back-action noise, respectively, and $\mu K(\Omega)$ is the optical rigidity. The relation between the Fourier transforms of the position x and the force F can be described as $\mu(-\Omega^2 + K(\Omega))x(\Omega) = F(\Omega)$. For simplicity we assume here that the measurement and the back-action noise are not correlated. Then the uncertainty relation is given by

$$S_F(\Omega)S_x(\Omega) \geq \hbar^2. \tag{2}$$

Substituting (2) in form $S_F(\Omega) \geq \hbar^2/S_x(\Omega)$ into (1) we can find the minimal value of the sensitivity $\xi(\Omega)$ (after optimization over S_x) which is better than the SQL

$$\xi^2_{\min}(\Omega) = \frac{|-\Omega^2 + K(\Omega)|}{\Omega^2} < 1 \tag{3}$$

in the bandwidth $\Delta\Omega$, where $|K(\Omega) - \Omega^2| < \Omega^2$, i.e. close to optical spring resonance. In other words a harmonic oscillator provides a gain in sensitivity for near-resonance signals, equal to

$$\xi^2 = \frac{\Delta\Omega}{\Omega} < 1. \tag{4}$$

Usually the two resonances are at two separate frequencies. The gain in sensitivity by means of the optical rigidity was examined in [28,29,32] for the wide-band regime under conditions $\Delta\Omega \sim \Omega$ and $\xi \gtrsim 1/2$.

The case of so-called *double resonance* [27,30,31], when an sophisticated frequency dependence of the optical rigidity allows us to obtain two close or coinciding resonance frequencies and to get better gain in sensitivity, is described by the following formula:

$$\xi^2 = \frac{S_h}{h^2_{\mathrm{SQL}}} = \left(\frac{\Delta\Omega}{\Omega}\right)^2. \tag{5}$$

It is important to note that the oscillatory sensitivity gain, described in Eq. (4), does not provide any gain in the signal to noise ratio in case the signal has a bandwidth larger than $\Delta\Omega$ (because the signal to noise ratio scales as the sensitivity gain multiplied by the bandwidth $\Delta\Omega$). However, for a double-resonance configuration with a sensitivity described by Eq. (5) the signal to noise ratio increases with decreasing bandwidth proportional to $\Delta\Omega^{-1}$ [27,30,31]. Please note that in the Advanced LIGO configuration optical rigidity can be created easily through microscopic position changes of the signal recycling mirror [28–31] as it is already being used in GEO 600 detector [6].

A single optical spring always causes instability (when there is no intrinsic mechanical damping). This can qualitatively be explained [23–25] by taking into account that the optical rigidity is not introduced instantaneously but with a delay of the relaxation time τ^* of the optical resonator. Therefore, the evolution of the free mass

position x with the optical rigidity K may approximately be described by the equation

$$m\ddot{x}(t) + Kx(t - \tau^*) = 0. \tag{6}$$

Expanding the second term in a series $x(t - \tau^*) \simeq x(t) - \tau^*\dot{x}(t)$ we can rewrite the previous equation in the form

$$m\ddot{x}(t) - K\tau^*\dot{x}(t) + Kx(t) = 0. \tag{7}$$

Obviously, the term $-K\tau^*\dot{x}$ corresponds to a negative damping force. Please note that in the opposite case of *negative* optical rigidity a *positive* damping force is introduced (the sign of the rigidity correlates with the sign of the detuning).

The instability (negative damping) can be compensated by incorporating a linear feedback control loop, and in the ideal case (no additional noise is introduced by the feedback) it would not modify the noise spectrum of a GW detector [29]. In practice, however, the need for control gain at frequencies inside the detection band can cause undesirable complexity in the control system or can introduce additional classical noise.

An alternative way to suppress the instability was proposed [33] and experimentally demonstrated [34] by injecting a second carrier field from the bright port (see Fig. 1) in order to create a relatively small additional negative rigidity component, thus the total rigidity (of both lasers together) remains positive, but at the same time introduce a relatively large additional positive damping component to make total damping positive. The main purpose of the second carrier is to create a second optical spring that forms a stable optical spring together with the first one—even though each individual optical spring, acting alone, would be unstable. Both carriers are assumed to have different polarizations, so that there is no direct coupling between the two fields (although they both directly couple to the mirrors).

In this paper we further analyze the stability of an optical spring created by a double pump. The regime of *stable* double resonance analyzed in this paper provides the possibility to decrease the bandwidth of the resonance curve dramatically and, hence, to increase the signal to noise ratio even for signals with a wide bandwidth (as formula (5) predicts). In Sec. II we formulate the simple criterion of stability, and we apply it to the regimes of stable double resonance in Sec. III. In addition we discuss the possibilities to observe these regimes using the experimental setups of the Gingin and Glasgow Prototype interferometers.

II. STABLE OPTICAL SPRING

In the following we use notations similar to the ones introduced in [28,35]. We consider an Advanced LIGO interferometer with a signal recycling mirror (SRM) having an amplitude reflectivity ρ and a power recycling mirror (PRM) as shown in Fig. 1. We assume the mirrors

to be without any optical losses. In addition, we suppose that both Fabry-Perot (FP) cavities in the east and north arms are identical, each input mirror featuring an amplitude transmittance $T \ll 1$ and a reflectivity $R = \sqrt{1 - T^2}$, while each end mirror is completely reflecting. The end and input mirrors have an identical mass m and in absence of the laser pumps they can move as free masses. The PRM is used only to increase the average power incident onto the beam splitter and we assume that no fluctuational fields from the laser (west arm) reach the detector in the south arm. The mean frequency of each pump $\omega_{1,2}$ is equal to one of the eigen-frequencies of the FP cavities. L is the distance between the mirrors in the arms (4 km for (Advanced) LIGO); l is the mean distance between the SR mirror and the beam splitter. We also introduce the following notations:

$$e^{i\Omega L/c} \simeq 1 + \frac{i\Omega L}{c}, \qquad \gamma_0 = \frac{cT^2}{4L}, \qquad (8)$$

$$\phi_{1,2} = \frac{(\omega_{1,2} + \Omega)l}{c} \simeq \frac{\omega_{1,2}l}{c}, \qquad (9)$$

$$\Gamma_{1,2} = \gamma_0 \frac{1 - \rho^2}{1 + 2\rho \cos 2\phi_{1,2} + \rho^2}, \qquad (10)$$

$$\Delta_{1,2} = \gamma_0 \frac{2\rho \sin 2\phi_{1,2}}{1 + 2\rho \cos 2\phi_{1,2} + \rho^2}. \qquad (11)$$

Here γ_0 is the relaxation rate of a single FP cavity, $\Delta_{1,2}$ are the detunings introduced by the SR mirror, $\Gamma_{1,2}$ are the relaxation rates of the differential modes of the interferometer for each pump. The frequency of the differential mode depends on the arm length difference $z = x_E - y_E - (x_N - y_N)$ and its bandwidth and detuning are controlled by position of SR mirror, which is described by phase advance $\phi_{1,2}$ arising from differential mode detuning ($\phi_{1,2} = 0$ corresponds to resonance). We assume that $\phi_{1,2}$ do not depend on Ω due to the small length l of the SR cavity: $l \ll L$. It is worthwhile noting that the detunings $\Delta_{1,2}$ and relaxation rates $\Gamma_{1,2}$ can differ for different pumps.

The mechanical evolution of the differential arm length $z = x_E - y_E - x_N + y_N$ (see notations on Fig. 1) in the frequency domain is described by

$$z = \Psi(\Omega)(F_1 + F_2 + F_s), \quad F_s = \mu \Omega^2 L h, \quad (12a)$$

$$\Psi(\Omega) = \frac{1}{\mu[-\Omega^2 + K_1(\Omega) + K_2(\Omega)]}, \quad \mu = \frac{m}{4}, \quad (12b)$$

$$K_{1,2} = \frac{8 I_{1,2} \omega_{1,2} \Delta_{1,2}}{cmL[(\Gamma_{1,2} - i\Omega)^2 + \Delta_{1,2}^2]}, \quad (12c)$$

where h is a dimensionless metric of a gravitational wave; Ψ is the mechanical susceptibility ($K_{1,2}$ are the frequency dependent spring coefficients created by the corresponding

laser pump); $I_{1,2}$ are the average optical arm cavity powers of the carrier 1 or 2 with the mean optical frequencies $\omega_{1,2}$; F_1, F_2 are the back-action forces caused by the first and second pump.

The eigen frequencies are solutions of the characteristic equation

$$\Psi(\Omega)^{-1} = 0. \qquad (13)$$

Roots corresponding to stable oscillations must have a negative imaginary part (as we assume the time dependence of position to be $\sim e^{-i\Omega t}$).

The Eq. (13) can be rewritten using the dimensionless susceptibility $\chi = \Psi m(\Gamma_1^2 + \Delta_1^2)/8$ (here $m(\Gamma_1^2 + \Delta_1^2)/8$ is a convenient multiplier):

$$\chi^{-1} = \frac{Y}{(2 - x^2 - igx)(2\eta - x^2 - i\nu g x)}, \qquad (14a)$$

$$Y = Y_r + igx Y_i, \qquad (14b)$$

$$Y_r = x^6 - [2(1 + \eta) + \nu g^2]x^4 + (4\eta + P + Q)x^2$$
$$\qquad - 2\eta P - 2Q, \qquad (14c)$$

$$Y_i = (1 + \nu)x^4 - 2(\eta + \nu)x^2 + \nu P + Q, \qquad (14d)$$

$$x \equiv \frac{\sqrt{2}\Omega}{\sqrt{\Gamma_1^2 + \Delta_1^2}}, \qquad g \equiv \frac{2\sqrt{2}\Gamma_1}{\sqrt{\Gamma_1^2 + \Delta_1^2}}, \qquad (14e)$$

$$P \equiv \frac{32\omega_1 I_1 \Delta_1}{mcL(\Gamma_1^2 + \Delta_1^2)^2}, \qquad Q \equiv \frac{32\omega_2 I_2 \Delta_2}{mcL(\Gamma_1^2 + \Delta_1^2)^2},$$

$$\eta \equiv \frac{\Delta_2^2 + \Gamma_2^2}{\Delta_1^2 + \Gamma_1^2}, \qquad \nu \equiv \frac{\Gamma_2}{\Gamma_1}. \qquad (14f)$$

We choose the dimensionless frequency x so that for a single pump (i.e. $Q = 0$) the double (unstable) resonance would take place at $x^2 \simeq 1$ if $P = 1$ [30] (in formal limit $g \to 0$ when susceptibility is a pure real value).

In order to find the eigen-frequencies one has to solve the equation $Y(x) = 0$ and to analyze for which conditions the roots are stable. Undoubtedly the roots of this equation can easily be obtained by applying numerical methods. However, starting from a set of input parameters (powers and detunings of each pump) the numerical solution will provide a set of frequencies with *arbitrary* imaginary parts. The problem is to identify the values of the system parameters that actually provide stable roots with negative imaginary parts. In the following we formulate a criterion which allows us in a quite easy way to properly estimate a set of parameters fulfilling our requirements.

In the general case, Y_r is a third order polynomial of x^2, so all of its roots (which we assume to be real) can be written in the form of $\pm x_j^{(0)}$ ($j = 1, 2, 3$). An example of Y_r as a function of x^2 is plotted on Fig. 2.

In order to apply a successive approximation method we assume that the values of the function Y_i are small in the regions close to the roots of Y_r. If this is the case, then the roots of the equation $Y(x) = 0$ can be found using the
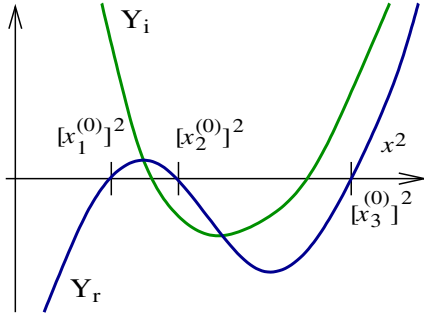
FIG. 2 (color online). Roots correspond to a stable (slightly damped) oscillation if Y'_r and Y_i have the same signs near roots of Y_r, i.e. plots of Y_r and Y_i correspond to each other as shown on plot.

successive approximations method taking 6 roots $\pm x_j^{(0)}$ of the equation $Y_r(x) = 0$ as a zeroth order approximation. In the first order approximation we add a small imaginary part to each root:

$$x_j = x_j^{(0)} + i\delta_j, \qquad x_j^{(0)} = \pm x_1^{(0)}, \qquad \pm x_2^{(0)}, \qquad \pm x_3^{(0)}. \tag{15}$$

After substituting this into Eq. (14b) we find δ_j:

$$Y'_r(x_j^{(0)})2x_j^{(0)}i\delta_j + igx_j^{(0)}Y_i(x_j^{(0)}) = 0,$$

$$\delta_j = -\left(\frac{g}{2}\right)\frac{Y_i(x_j^{(0)})}{Y'_r(x_j^{(0)})} < 00,$$

$$\text{where } Y'_r(x_j^{(0)}) \equiv \frac{dY_r}{d(x^2)}\bigg|_{x^2=(x_j^{(0)})^2}. \tag{16}$$

In order to fulfill the condition for a stable oscillation, δ_j have to be negative as we required in (16) [recall, as we assume the time dependence of position to be $\sim e^{-i\Omega t}$, hence, eigen frequency (x_j) corresponds to oscillations $\sim e^{-ix_j t}$ and negative imaginary part means damping]. Therefore, stable roots with $\delta_j < 0$ will be achieved in the case when the functions Y'_r and Y_i have the *same signs* in the regions close to roots of Y_r, i.e. their plots have to relate to each other as shown on Fig. 2.

We would like to emphasize that the obtained criterion is very simple and that it allows us to estimate whether a certain set of input parameters can provide roots (complex frequencies) with imaginary parts of the desired signs without the need to solve the characteristic equation. The proposed criterion is very close to the Routh-Hurwitz criteria [36]; however, it is more obvious and more useful for the particular analysis of optical spring stability.

The stability criterion described in Eq. (16) can easily be generalized for a larger number of optical pumps. For example, for three pumps the functions Y_r and Y_i are parabolas of fourth and third order correspondingly (in respect to x^2), and the roots will be stable if the functions
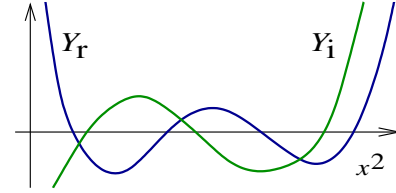

FIG. 3 (color online). For the case of 3 pumps the roots are stable if in accordance with criterion (16) the plots of Y_r and Y_i correspond to each other as shown.

Y'_r and Y_i have the same sign at the regions close to the roots of Y_r as shown in Fig. 3.

Obviously, the regimes of stable optical spring considered in [33] fulfil the condition described in Eq. (16). However, our criterion might be useful to identify configurations that can be experimentally implemented avoiding any feedback or for other interesting regimes such as double resonance or negative inertia [37].

III. STABLE DOUBLE RESONANCE

Oscillators in the double-resonance regime have interesting properties. The resonant force, with the time dependence $f = F_0 \cos\Omega_{\rm res}t$, acting on such an oscillator produces a displacement $z_{\rm dr} = -F_0 t^2/(8m)\cos\Omega_{\rm res}t \sim t^2$, which is much larger than the resonant displacement $z_{\rm co} = -F_0 t/(2m)\sin\Omega_{\rm res} \sim t$ of a conventional oscillator under action of the same force [30]. In the frequency domain the resonant gain of a conventional oscillator is $\sim \Omega_{\rm res}/\Delta\Omega$ (i.e. inverse proportional to the bandwidth $\Delta\Omega$ of the resonance curve), whereas the resonant gain of an oscillator in the double-resonance regime is much larger: $\sim (\Omega_{\rm res}/\Delta\Omega)^2$ (i.e. inverse proportional to the *square* of the bandwidth $(\Delta\Omega)^2$). This feature, as mentioned in the introduction, is responsible for the wide bandwidth gain in signal to noise ratio.

The double resonance takes place if the susceptibility has a pole of second order [27,30]. In terms of our stability criterion this means for the case of the double resonance that the plot of Y_r as function of x^2 touches the horizontal axis at the resonance frequency x_0^2 and Y_i is equal to zero at this point. Figure 4 illustrates two possible ways of behavior of Y_i: in Fig. 4(a) and 4(b) Y_i crosses and touches the
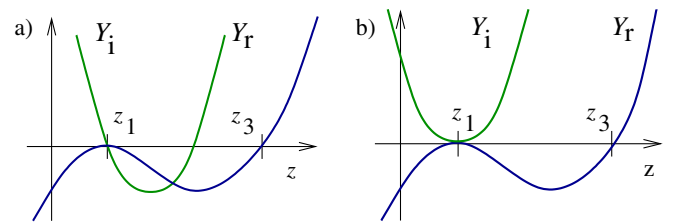

FIG. 4 (color online). "Ideal" double resonance: curve Y_r touches z axis in point z_1: a) left root $\bar{z}_1$ of Y_i coincides with z_1; b) curve Y_i touches z axis in the same point z_1.
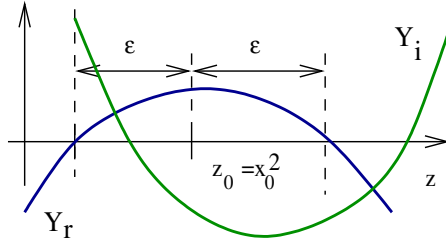
FIG. 5 (color online). Detailed plot of two close roots of Y_r (14c). The roots of Y_i (14d) have to be shifted to the right relative to the roots of Y_r in order to fulfill the stability criterion (16).
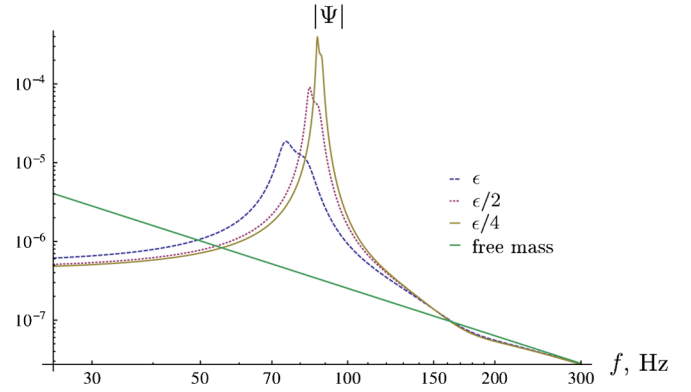

FIG. 6 (color online). Trace 1: susceptibility $|\Psi(f)|$ as function of frequency $f = \Omega/2\pi$ for the parameters given in Eq. (19). Traces 2,3: same as trace 1 but with $\epsilon \rightarrow \epsilon/2$ and with $\epsilon \rightarrow \epsilon/4$. Trace 4: susceptibility of free mass $(4/m(2\pi f)^2)$.

horizontal axis at $x^2 = x_0^2$, respectively. However, it is difficult to exactly realize the regimes shown in Fig. 4— some discrepancies like shown on Fig. 2 are inevitable.

In general, double resonance takes place when any two of three roots $[x_1^{(0)}]^2$, $[x_2^{(0)}]^2$, $[x_3^{(0)}]^2$ coincide. In this section we consider the particular case of close smaller roots $[x_1^{(0)}]^2$, $[x_2^{(0)}]^2$ of Y_r (our preliminary analysis shows that the other case of close roots $[x_2^{(0)}]^2$, $[x_3^{(0)}]^2$ can not provide a stable set of roots):

$$[x_{1,2}^{(0)}]^2 \simeq x_0^2 \pm \epsilon, \qquad \epsilon \ll 1, \qquad (17)$$

where x_0^2 is a middle point between the roots $[x_{1,2}^{(0)}]^2$. Hence, Y_r may be presented in the form

$$Y_r = (x^2 - x_0^2 - \epsilon)(x^2 - x_0^2 + \epsilon)(x^2 - [x_3^{(0)}]^2). \quad (18)$$

In order to fulfill the criterion (16) one has to arrange the parabolas along the x^2 axis in such a way that the roots of Y_i would be placed close to roots of Y_r (see Fig. 5). Shifting Y_i along the vertical axis allows us to manipulate the damping at the resonant frequencies because the values of Y_i at the roots of Y_r define the mechanical damping of the oscillator (16). The problem of properly arranging this two curves is solvable as there are enough parameters for manipulation available: the two detunings and the two powers of the two pumps (i.e. the dimensionless parameters P, Q, η, ν). An example of a step by step calculation is

presented in Appendix A. For the following dimensionless parameters

$$P \simeq 0.77, \quad Q \simeq -0.027, \quad g = 0.6, \quad d \simeq 1.39, \quad (19a)$$
$$\eta \simeq 0.24, \quad \nu = 0.5, \quad \epsilon = 0.05, \quad (19b)$$

we get the eigen-frequencies

$$\Omega_1 \simeq 532.3 \text{ s}^{-1}, \qquad \delta_1 \simeq 16.8 \text{ s}^{-1}, \qquad (20)$$
$$\Omega_2 \simeq 482.1 \text{ s}^{-1}, \qquad \delta_2 \simeq 15.4 \text{ s}^{-1}, \qquad (21)$$
$$\Omega_3 \simeq 961.8 \text{ s}^{-1}, \qquad \delta_3 \simeq 314.2 \text{ s}^{-1}. \qquad (22)$$

Using Advanced LIGO parameters as listed in Table I the set (19) can be recalculated, giving the following results:

$$\Gamma_1 \simeq 230 \text{ s}^{-1}, \qquad \Delta_1 \simeq 1063 \text{ s}^{-1}, \qquad I_1 \simeq 863 \text{ kW},$$
$$\Gamma_2 \simeq 115 \text{ s}^{-1}, \qquad \Delta_2 \simeq -526 \text{ s}^{-1}, \qquad I_2 \simeq 61 \text{ kW},$$
$$(\phi_1 \simeq 1.49, \phi_2 \simeq -1.39).$$

Figure 6 shows the corresponding susceptibility Ψ^{-1} as a function of frequency $f = \Omega/2\pi$ for the listed parameters. It is worth emphasizing that it is possible to realize a stable double resonance with *arbitrary small* damping by just choosing smaller values for ϵ. Figure 6 includes the susceptibility for several values of parameter ϵ: $\epsilon \rightarrow \epsilon/2, \epsilon/4$, as well as the susceptibility of the free masses as comparison.

IV. Possibilities of experimental observation

It would be interesting to demonstrate and observe unusual high susceptibility in stable double-resonance regime experimentally (it should be proportional to $\Delta\Omega^{-2}$ but not to $\Delta\Omega^{-1}$ as in conventional resonance). For example, this could be done in Gingin High Optical Power Test Facility [38]. The initial formulas (14) are valid for the Gingin topology with one exception. Only one arm of the

TABLE I. Parameters of Advanced LIGO used in this paper.

Parameter	Value
Arm length, L	4 km
Mass of each mirror, m	40 kg
IM amplitude transmittance, T	$\sqrt{0.005}$
Relaxation rate of single FP cavity, γ_0 (8)	94 s^{-1}
SRM amplitude reflectivity ρ	$\sqrt{0.93}$
Optical wavelength, λ	1064 nm

Michelson interferometer (with Fabry-Perot arm cavities) is used in Gingin; hence, one has to define the power parameters P and Q a factor 2 smaller:

$$P \equiv \frac{16k_1 I_1 \Delta_1}{mL(\Gamma_1^2 + \Delta_1^2)^2}, \qquad Q \equiv \frac{16k_2 I_2 \Delta_2}{mL(\Gamma_1^2 + \Delta_1^2)^2}. \quad (23)$$

The Gingin facility features test masses of $m = 0.8$ kg and arm length is $L = 80$ m. Then, assuming $\Gamma_1 = 400$ s^{-1}, it is easy to recalculate the parameters (19) for Gingin:

$$\Gamma_1 \simeq 400 \text{ s}^{-1}, \qquad \Delta_1 \simeq 843 \text{ s}^{-1}, \qquad I_1 \simeq 3.59 \text{ kW},$$
$$(24)$$

$$\Gamma_2 \simeq 200 \text{ s}^{-1}, \qquad \Delta_2 \simeq -911 \text{ s}^{-1}, \qquad I_2 \simeq 0.254 \text{ kW}.$$
$$(25)$$

It seems that these parameters may be relatively easy realized using the Gingin facility.

Another experimental setup that can be used to observe a stable double resonance is the Glasgow 10 m Prototype [39,40]. In contrast to the balanced scheme of a full Michelson interferometer such as Advanced LIGO, where it is possible to pump the interferometer with the *symmetric* mode tuned to resonance, while observing the optical rigidity in the *antisymmetric* mode, in the Glasgow Prototype (shown on Fig. 7) the same mode will have to be used to pump and to observe rigidity. Recall that the smaller the detuning the larger is the circulating power, whereas optical rigidity requires a large detuning. However, it is possible to set the first cavity between PRM and input mirror (IM) to antiresonance (the relaxation rates $\Gamma_1 = \Gamma_2 = T_{PRM}T_{IM}c/4L$ reach their minimum) and to create the detuning by shifting the position of the end mirror. In this situation the Eqs. (14) can be used with $\nu = 1$. Taking into account that practically only the light end mirror can move the power parameters P, Q have to be redefined, reduced by factor 4:

$$P \equiv \frac{8k_1 I_1 \Delta_1}{mL(\Gamma_1^2 + \Delta_1^2)^2}, \qquad Q \equiv \frac{8k_2 I_2 \Delta_2}{mL(\Gamma_1^2 + \Delta_1^2)^2}. \quad (26a)$$
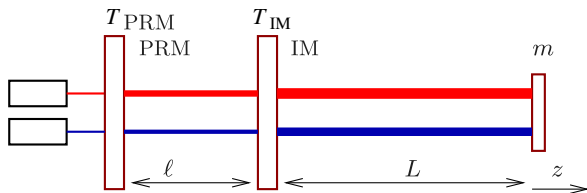

FIG. 7 (color online). Scheme of the optical rigidity experiment within the Glasgow Prototype Interferometer. Only the end mirror can move, while the mirrors PRM and IM can be considered as unmovable because their masses are 30 times larger than that of the end mirror.

Then we can apply the scheme presented in Appendix A. In particular the stable double resonance is characterized by the following set of dimensionless parameters:

$$P \simeq 2.43, \quad Q \simeq -0.51, \quad g = 0.625, \quad d \simeq 1.27, \quad (27a)$$
$$\eta \simeq 0.71, \quad \nu = 1, \quad \epsilon = 0.01. \quad (27b)$$

Using the actual parameters of the Glasgow Prototype, as presented in Table II, we can calculate the following set of experimental parameters:

$$\Gamma_1 = \Gamma_2 \simeq 937 \text{ s}^{-1},$$
$$\Delta_1 \simeq 4138 \text{ s}^{-1},$$
$$\Delta_2 \simeq -3450 \text{ s}^{-1}, \quad (28)$$
$$I_{1\,\text{input}} \simeq 1.28 \text{ W},$$
$$I_{2\,\text{input}} \simeq 0.33 \text{ W}.$$

Here $I_{1\,\text{input}}$, $I_{2\,\text{input}}$ are the input powers of the two pump lasers.

Unfortunately, the observation of a stable double resonance is more difficult for smaller scale experiments. For example, one may consider an experimental setup as described in [34] of a short Fabry-Perot cavity (without power recycling) and a light-weight movable mirror: the power transmittance of the input mirror is $T^2 = 0.8 \times 10^{-3}$, the distance between the mirrors is $L \simeq 0.9$ m, and the mass of the movable mirror is $m = 1$ g. Then the dimensionless parameters (27) can be recalculated as follows:

$$\Gamma_1 = \Gamma_2 \simeq 66.7 \times 10^3 \text{ s}^{-1}, \quad (29)$$

$$\Delta_1 \simeq 294 \times 10^3 \text{ s}^{-1}, \qquad \Delta_2 \simeq -245 \times 10^3 \text{ s}^{-1}, \quad (30)$$

$$I_{1\,\text{input}} \simeq 2.64 \text{ kW}, \qquad I_{2\,\text{input}} \simeq 1.26 \text{ kW}. \quad (31)$$

Obviously these input power values are impermissibly huge to be realized in an experiment. In order to find some regularities concerning the experiment scale we can rewrite the formula (26) in the following form using the value of input power:

TABLE II. Parameters of Glasgow Prototype Interferometer.

Parameter	Value
Arm length, L	10 m
Distance between PRM and IM, ℓ	5 m
Mass of movable mirror, m	100 g
Masses of PRM and IM, M	3 kg
PRM amplitude transmittance T_{PRM}	$\sqrt{0.05}$
IM amplitude transmittance, T_{IM}	$\sqrt{0.01}$
Input power, I_{input}	≥ 1 W,
Optical wavelength, λ	1064 nm

$$P = \left(\frac{8k_1 L^2 I_{1\,\text{input}}}{mc^3(T_{\text{eff}}/4)^4}\right) \times \frac{\Delta_1/\Gamma_1}{(1 + \Delta_1^2/\Gamma_1^2)^3} \propto \frac{L^2 I_{1\,\text{input}}}{mT_{\text{eff}}^4}, \quad (32)$$

where we substitute $\Gamma_1 = T_{\text{eff}}^2 c/4L$. For the Glasgow prototype the effective transmittance is equal to $T_{\text{eff}} = T_{\text{PRM}}T_{\text{IM}}/4$.

In order to find out whether an experiment is realizable, we emphasized in expression (32) only the proportionality to the terms, which significantly change with changes of the experiment scale. Decreasing the scale of the experiment is usually represented by decreasing the mass m of the movable mirror and the distance L between the mirrors, which approximately compensate each others contribution into P. That means that in order to achieve the needed value of P and thus to observe the desired stable double resonance one needs to keep the effective transmittance roughly the same as in a bigger scale experiment due to the strong dependence of P on T_{eff}. This leads to the need for the circulating power to be the same as for the bigger scale experiment, which would be pretty difficult due to problems caused by absorption induced heating of the small mirror.

V. CONCLUSION AND OUTLOOK

We developed a new criterion for the stability of an optical spring and applied it to the double-resonance scheme. Before such a concept can be realized in a large-scale gravitational-wave detector it would be beneficial to demonstrate it on a prototype scale experiment, such as the Glasgow Prototype [39,40], Gingin High Optical Power Test Facility [38], or the AEI 10 m Prototype Interferometer [41].

It is worth noting that our criterion for optical spring stability may also be applied to the negative inertia regime recently proposed by F. Ya. Khalili and colleagues [37] (the term "negative inertia" was proposed earlier by H. Müller-Ebhardt [42]). This directly follows from the fact that the negative inertia scheme formally corresponds to a double-resonance configuration with a resonance frequency of zero.

The formulated stability criterion is also valid for gravitational-wave detectors pumped by more than two lasers. This may allow us to realize *stable triple (or quadro)* resonance, i.e. regimes when three (or four) eigen-frequencies coincide or are close to each other. In this case the response to force at the resonance frequency is greater than for a double-resonance configuration. In the frequency domain the resonant gain for a triple resonance has to be proportional to $\sim(\Omega_{\text{res}}/\Delta\Omega)^3$ [i.e. inverse proportional to the *third* power of the bandwidth $(\Delta\Omega)^3$]. It will allow us to further increase the gain in the signal to noise ratio for wide bandwidth signals, mentioned in the Introduction, by a factor $\Omega_{\text{res}}/\Delta\Omega$ compared to the double resonance. In this paper no sensitivity analysis for gravitational detectors was performed, but we plan to do this in a future publication.

A stable double resonance featuring arbitrarily large susceptibility may allow us to use it for the production of squeezed light by means of the ponderomotive nonlinearity [34,43]. However, the obtained squeezing will have specific features [33]: One would have to measure two optimal quadratures, corresponding to each carrier, and squeezing can only be observed by finding their correct combination because they are correlated (entangled) through the mechanical degree of freedom.

Because of the combination of a uniquely large susceptibility and a low noise level the stable double (or triple) resonance may also be applied to macroscopic quantum mechanics experiments with mirrors of relatively small mass. In particular, it can be used for the observation of quantum entanglement between an oscillator and an electro-magnetic field [44,45] or for preparation of the mechanical oscillator in a nongaussian quantum state [46].

In addition stable double resonance may be a useful instrument in other precision measurements in order to increase mechanical transduction. For example, double-resonance regime may be applied to the measurements of thermal noise of mirror coatings. In case the mass m of one cavity mirror is small enough compared to the other one, the equation for the variation z of the optical distance inside the cavity may be written in the frequency domain as follows:

$$m(-\Omega^2 + K(\Omega))z = F_{\text{ba}} - m\Omega^2 z_{\text{th}}, \quad (33)$$

where z_{th} are the thermal fluctuations of the mirror surface in respect to the mirror's center of mass and F_{ba} is the back-action force. Homodyne detection of the output wave yields the information on z. One can obtain resonant gain of the signal (in this case it is z_{th}) inside the resonance bandwidth (i.e. for $\Omega = \Omega_{\text{res}} \pm \Delta\Omega/2$) and in case of a stable double resonance this gain is unusually large.

ACKNOWLEDGMENTS

APPENDIX A: DETAILS OF THE DOUBLE-RESONANCE STABILITY ANALYSIS

In this appendix we present the example estimation of a set of input parameter values needed to realize the regime of a stable double resonance. We will deal mainly with the functions Y_r and Y_i in this section. As it was mentioned in Sec. III we need to arrange these parabolas along the x axis to achieve close stable frequencies and then arrange the

parabola Y_i along the y axis to obtain the desired values of the imaginary parts of the frequencies or, other words, the desired bandwidth of the double resonance.

First, we assume the two smaller roots of Y_r to be close enough to each other. That means that the function Y_r can be expressed in form (19)

$$Y_r = (z - z_0 - \epsilon)(z - z_0 + \epsilon)(z - z_3), \qquad z \equiv x^2, \tag{A1}$$

where 2ϵ is the distance between the close roots (and ϵ is small). We also introduce the parameter $d = z_3 - z_0$ which is defined as the distance between the center of the two close roots and the "lonely" root.

Proper substitution transforms this cubic function into the reduced form $Y_r = y^3 + py + q$. In our case the substitution is $z = y + (2z_0 + z_3)/3$. The particular case of this equation with $z = z_0$ and $y = y_0$ (y_0 is the middle of the close roots in terms of the shifted variable) leads us to the following equation:

$$y_0 = -\frac{z_3 - z_0}{3} = -\frac{d}{3}. \tag{A2}$$

After the substitution is done the parameters p and q are expressed in terms of ϵ and d as follows:

$$p = -\frac{1}{3}d^2 - \epsilon^2, \qquad q = -\frac{2}{27}d(d^2 - 9\epsilon^2). \tag{A3}$$

On the other hand the function Y_r is expressed (14c) in terms of the input parameters such as the pump powers and the detunings (parameters P, Q, g, η, ν). Substitution of

$$y = z + \frac{2(1 + \eta) + \nu g^2}{3}$$

transforms the function into the familiar form $Y_r = y^3 + py + q$. However, this time the coefficients p and q are expressed in terms of the above mentioned input parameters.

Equating the pairs of expressions for p and q (expressed in different terms) one can obtain the solutions for the pump powers P and Q as functions of the remaining input parameters as well as ϵ and d.

At this step the x arrangement of the function Y_r is completed. Indeed, if we set a certain value of d we can expect the middle of the close roots (in the shifted variables) to be equal to $-d/3$. Setting a certain value of ϵ results in the close roots to be separated by 2ϵ.

The next step is to arrange Y_i thus it provides stability of the complex frequencies. According to the stability criterion (16) frequencies are expected to be stable if the roots of Y_r (z_1, z_2) and Y_i ($\bar{z}_1$, $\bar{z}_2$) are located in the same way as is shown on Fig. 8:

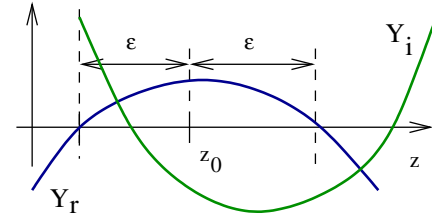$$z_1 < \bar{z}_1, \qquad z_2 < \bar{z}_2. \tag{A4}$$

FIG. 8 (color online). Detailed plot of the two close roots of Y_r (14c): $z_{1,2} = z_0 \pm \epsilon$. The roots of Y_i (14d) are separated by the same distance 2ϵ, but the trace of Y_i itself is shifted by the distance ϵ_1.

The values $z_{1,2}$ can be estimated using Cardano's formulae (see Appendix B), and $\bar{z}_{1,2}$ are the roots of a quadratic equation:

$$z_{1,2} \simeq -\left(-\frac{q}{2}\right)^{1/3} + \frac{2(1 + \eta) + \nu g^2}{3} \mp \epsilon,$$

$$\bar{z}_{1,2} = \frac{\nu + \eta}{1 + \nu} \mp \sqrt{\left(\frac{\nu + \eta}{1 + \nu}\right)^2 - \frac{\nu P + Q}{1 + \nu}}.$$

After properly arranging Y_i thus it complies with the condition (A4) the second step is completed. We obtained three stable frequencies, two of which are separated by the desired distance of 2ϵ.

It is obvious that in order to obtain a single resonance peak, one should choose a distance between the close frequencies smaller than the mean imaginary part of these roots δ_j. Since $z = x^2$, the distance between the close frequencies can be estimated as $x_2 - x_1 \sim \epsilon/\sqrt{z_0}$. Equation (16) gives an estimate for δ. Summing this up one can write

$$\frac{\epsilon}{\sqrt{z_0}} \lesssim \left|\frac{gY_i(z_{1,2})}{2Y_r'(z_{1,2})}\right| \simeq \left|\frac{gY_i(z_{1,2})}{4\epsilon d}\right|,$$

or

$$|Y_i(z_{1,2})| \geq \frac{4\epsilon^2 d}{g_1\sqrt{z_0}}. \tag{A5}$$

For us regimes with infinitely close frequencies, i.e. with $\epsilon \to 0$, are of interest. Along with decreasing the distance between frequencies we can also decrease the bandwidth of the double resonance or in other words the values of δ_j, which is possible by decreasing the values of Y_i. Equation (A5) is the only condition these values should obey.

To ensure this we apply the following conditions to the values of Y_i:

$$Y_i(z_1) = s_1 \frac{4\epsilon^2 d}{g_1\sqrt{z_0}}, \qquad Y_i(z_2) = -s_2 \frac{4\epsilon^2 d}{g_1\sqrt{z_0}}, \tag{A6}$$

where the variables s_1 and s_2 are subject to fitting and should be approximately equal to unity. This is the final step, resulting in a set of three stable frequencies, two of

which form the resonant peak of the desired bandwidth in the susceptibility.

It is worth noting that the parameter ϵ is proportional to distance the between the roots of Y_r, and, hence, ϵ is proportional to the bandwidth of the resonance. The parameters g, ν are free and can be used to vary the resonance frequencies or the values of the pumping powers.

APPENDIX B: CUBIC EQUATION: CARDANO'S FORMULA

The cubic equation

$$x^3 + ax^2 + bx + c = 0 \tag{B1}$$

may be written in the depressed cubic form by substitution of $x = y - a/3$ [36]:

$$0 = y^3 + py + q, \tag{B2}$$

$$p = -\frac{a^2}{3} + b, \qquad q = 2\left(\frac{a}{3}\right)^3 - \frac{ab}{3} + c. \tag{B3}$$

The roots of this depressed cubic equation are given by

$$y_{1,2} = -\frac{A+B}{2} \pm i\sqrt{3}\frac{A-B}{2}, \quad y_3 = A + B, \tag{B4a}$$

$$\text{where } A = \left(-\frac{q}{2} + \sqrt{D}\right)^{1/3}, \quad B = \left(-\frac{q}{2} - \sqrt{D}\right)^{1/3}, \tag{B4b}$$

$$D = \left(\frac{p}{3}\right)^3 + \left(\frac{q}{2}\right)^2. \tag{B4c}$$

For A and B one should choose any cubic roots from the corresponding expressions, which fulfill the following equation:

$$AB = -p/3. \tag{B5}$$

In case this equation has real coefficients one should take the real values of the roots (if possible).

---

[1] A. Abramovici *et al.*, Science **256**, 325 (1992).
[2] D. Sigg *et al.*, Classical Quantum Gravity **23**, S51 (2006).
[3] LIGO website, http://www.ligo.caltech.edu.
[4] F. Acernese *et al.*, Classical Quantum Gravity **23**, S635 (2006).
[5] VIRGO website, http://www.virgo.infn.it.
[6] H. Luck *et al.*, Classical Quantum Gravity **23**, S71 (2006).
[7] GEO-600 website, http://geo600.aei.mpg.de.
[8] M. Ando *et al.*, Classical Quantum Gravity **22**, S881 (2005).
[9] TAMA-300 website, http://tamago.mtk.nao.ac.jp.
[10] D. E. McClelland *et al.*, Classical Quantum Gravity **23**, S41 (2006).
[11] ACIGA website, http://www.anu.edu.au/Physics/ACIGA.
[12] A. Weinstein, Classical Quantum Gravity **19**, 1575 (2002).
[13] Advanced LIGO website, https://www.advancedligo.mit.edu/.
[14] Advanced Virgi website, wwwcascina.virgo.infn.it/advirgo/.
[15] B. Willke, Classical Quantum Gravity **23**, S207 (2006).
[16] K. Kuroda, Classical Quantum Gravity **23**, S215 (2006).
[17] V. B. Braginskii, Sov. Phys. JETP **26**, 831 (1968).
[18] V. B. Braginsky and Yu. I. Vorontsov, Sov. Phys. Usp. **17**, 644 (1975).
[19] V. B. Braginsky, Yu. I. Vorontsov, and F. Ya. Khalili, Zh. Eksp. Teor. Fiz. **73**, 1340 (1977)[Sov. Phys. JETP **46**, 705 (1977)].
[20] V. B. Braginsky and F. Ya. Khalili, *Quantum Measurement* (Cambridge University Press, Cambridge, 1992).
[21] M. Punturo, M. Abernathy, F. Acernese, B. Allen, N. Andersson, K. Arun, F. Barone, B. Barr, M. Barsuglia,

M. Beker *et al.*, Classical Quantum Gravity **27**, 084007 (2010).
[22] S. Hild, S. Chelkowski, A. Freise, J. Franc, N. Morgado, R. Flaminio, and R. DeSalvo, Classical Quantum Gravity **27**, 015003 (2010).
[23] V. B. Braginsky and I. I. Minakova, Vestnik Moskovskogo Universiteta, Fizika i Astronomiya (in Russian) **1**, 83 (1967).
[24] V. B. Braginsky and A. B. Manukin, Zh. Eksp. Teor. Fiz. **52**, 986 (1967)[Sov. Phys. JETP **25**, 653 (1967).]
[25] V. B. Braginskii, National Aeronautics and Space Administration, F-672, 1972.
[26] V. B. Braginsky and F. Ya. Khalili, Phys. Lett. A **257**, 241 (1999).
[27] F. Ya. Khalili, Phys. Lett. A **288**, 251 (2001).
[28] A. Buonanno and Y. Chen, Phys. Rev. D **64**, 042006 (2001).
[29] A. Buonanno and Y. Chen, Phys. Rev. D **65**, 042001 (2002).
[30] V. I. Lazebny and S. P. Vyatchanin, Phys. Lett. A **344**, 7 (2005).
[31] F. Ya. Khalili, V. I. Lazebny, and S. P. Vyatchanin, Phys. Rev. D **73**, 062002 (2006).
[32] A. Buonanno and Y. Chen, Phys. Rev. D **69**, 102004 (2004).
[33] H. Rehbein, H. Müller-Ebhardt, K. Somiya, S. L. Danilishin, R. Schnabel, K. Danzmann, and Y. Chen, Phys. Rev. D **78**, 062003 (2008).
[34] T. Corbitt, Y. Chen, E. Innerhofer, H. Müller-Ebhardt, D. Ottaway, H. Rehbein, D. Sigg, S. Whitcomb, C. Wipf, and N. Mavalvala, Phys. Rev. Lett. **98**, 150802 (2007).

[35] H. J. Kimble, Yu. Levin, A. B. Matsko, K. S. Thorne, and S. P. Vyatchanin, Phys. Rev. D **65**, 022002 (2001).

[36] G. A. Korn and T. M. Korn, *Mathematical Handbook* (Mc-Graw-Hill, New York, 1968).

[37] Y. Chen, S. Danilishin, F. Khalili, H. Miao, H. Müller-Ebhardt, C. Zhao, Report No. LIGO-T1000069, 2010.

[38] C. Zhao *et al.*, J. Phys. Conf. Ser. **32**, 368 (2006).

[39] S. H. Huttner, B. W. Barr, M. V. Plissi, J. R. Taylor, B. Sorazu, and K. A. Strain, Classical Quantum Gravity **24**, 3825 (2007).

[40] M. P. Edgar, B. W. Barr, J. Nelson, M. V. Plissi, K. A. Strain, O. Burmeister, M. Britzger, K. Danzmann, R. Schnabel, T. Clausnitzer *et al.*, Opt. Lett. **34**, 3184 (2009).

[41] S. Gossler, A. Bertolini, M. Born, Y. Chen, K. Dahl, D. Gering, C. Gräf, G. Heinzel, S. Hild, F. Kawazoe, O.

Kranz, G. Kühn, H. Lück, K. Mossavi, R. Schnabel, K. Somiya, K. A. Strain, J. R. Taylor, A. Wanner, T. Westphal, B. Willke, and K. Danzmann, Classical Quantum Gravity **27**, 084023 (2010).

[42] H. Müller-Ebhardt, Ph.D. thesis University of Hannover, 2008.

[43] T. Corbitt, Y. Chen, F. Khalili, D. Ottaway, S. Vyatchanin, S. Whitcomb, and N. Mavalvala, Phys. Rev. A **73**, 023801 (2006).

[44] H. Miao, S. Danilishin, and Y. Chen, Phys. Rev. A **81**, 052307 (2010).

[45] H. Miao, S. Danilishin, H. Müller-Ebhardt, H. Rehbein, K. Somiya, and Y. Chen, Phys. Rev. A **81**, 012114 (2010).

[46] F. Khalili, S. Danilishin, H. Miao, H. Müller-Ebhardt, H. Yang, and Y. Chen, Phys. Rev. Lett. **105**, 070403 (2010).